IEEE Access
Multidisciplinary ⋮ Rapid Review ⋮ Open Access Journal

Received February 5, 2021, accepted February 22, 2021, date of publication February 24, 2021, date of current version March 9, 2021.

Digital Object Identifier 10.1109/ACCESS.2021.3062075

Performance of Ge and $In_{0.53}Ga_{0.47}As$ Thermophotovoltaic Cells under Different Spectral Irradiances

MANSUR MOHAMMED ALI GAMEL[1], PIN JERN KER[1], (Member, IEEE), WAN EMILIN SULIZA WAN ABDUL RASHID[2], (Member, IEEE), HUI JING LEE[3], (Member, IEEE), M. A. HANNAN[2], (Senior Member, IEEE), AND MD. ZAINI BIN JAMALUDIN[2], (Senior Member, IEEE)

[1]Institute of Sustainable Energy, Universiti Tenaga Nasional, Kajang 43000, Malaysia
[2]Institute of Power Engineering, Universiti Tenaga Nasional, Kajang 43000, Malaysia
[3]Department of Electrical and Electronics Engineering, College of Engineering, Universiti Tenaga Nasional, Kajang 43000, Malaysia

Corresponding author: Pin Jern Ker (pinjern@uniten.edu.my)

This work was supported in part by the Tenaga Nasional Berhad (TNB) seeding fund, that is managed by the UNITEN R&D Sdn. Bhd., under Project U-TG-RD-18-04, and in part by the Building Opportunities, Living Dreams (BOLD) Refresh Publication Fund 2021 under Grant J5100D4103.

ABSTRACT The investigation on the effect of illumination power intensities for a thermophotovoltaic (TPV) system is crucial to enhance the TPV cell performance. To date, the studies on the effect of illumination intensities were limited to solar photovoltaic cells application. Meanwhile, the reported work on the impact of infrared illumination intensities on TPV cells are done at limited temperatures and intensities. The effects of TPV intensities on all performance parameters are not comprehensively studied and fully elucidated. Therefore, this paper investigates the performance of indirect-bandgap Germanium (Ge) and direct-bandgap Indium Gallium Arsenide (InGaAs) cells under various TPV spectral irradiances. Silvaco TCAD simulation software was used to investigate the effect of blackbody temperatures ranging from 800 to 2000 K with different illumination intensities on the TPV cell performances. It was found that higher conversion efficiencies are achieved for both TPV cells under higher illumination intensities due to the increase in open-circuit voltage and fill factor. As the beam intensity increases for temperatures >1600 K, fill factor slowly increases for the Ge cell, but decreases for the InGaAs cell due to the increase in the I^2R_s losses associated with the high current. The finding demonstrates that the open-circuit voltage of indirect-bandgap TPV cell is significantly increased with higher illumination intensities. The variations in cells performance are explicitly explained based on factors such as TPV design structure and the physical properties of semiconductor at varying illumination intensities. The performance of both TPV cells were also analyzed at the minimum optical losses. Average efficiencies of Ge and InGaAs TPV cells were increased to 26.05% and 27.92%, respectively, when the optical losses were minimized with anti-reflection coating and thicker absorber layer. The results of this work demonstrate that by detailed consideration of the effect of spectral irradiances, a high-performance TPV system can be developed.

INDEX TERMS Energy conversion, Ge, InGaAs, spectral irradiances, thermophotovoltaic.

I. INTRODUCTION

Over the past decades, thermophotovoltaic (TPV) system has emerged as a promising technology for the energy conversion of thermal radiations such as fuel combustion, waste heat recovery, and nuclear energy, into electricity. The TPV systems have been realized in many applications such as off-grid electrical generator [1], [2], aerospace applications [1], vehicle [3], submarine [4], solar thermophotovoltaic (STPV) [5], [6], energy storage [7], [8] and waste heat recovery systems in metal-alloy industries [2], [9], [10], power plant [11], [12] and fuel cell [13]. The typical source of

The associate editor coordinating the review of this manuscript and approving it for publication was Leo Spiekman.

temperature for thermal radiation in TPV applications is less than 2000 K. In terms of the operating principle, TPV cells operate similar to solar cells, which can absorb the thermal radiations from a heat source and convert them into electricity. Unlike solar cells, TPV cells require a narrower bandgap (NB) semiconductor such as Germanium (Ge) and Indium Gallium Arsenide ($In_{0.53}Ga_{0.47}As$), herein after referred to as InGaAs, to convert the infrared radiations (IRs).

In comparison to InGaAs, Ge has lower absorption coefficient because it is an indirect bandgap material [14]. However, Ge is relatively abundant in supply and rather a cost-effective material to fabricate TPV cells [15], [16]. On the other hand, InGaAs is a direct III–V semiconductor material that has excellent optical and electrical properties, such as strong light absorption, high diffusion coefficient, long carrier lifetime, and large carrier diffusion length [17], [18]. On top of that, the maturity of InGaAs and monolithic interconnected module (MIM) lattice-matched to the available indium phosphide (InP) substrate makes it a suitable candidate for large-scale production [19]. Nevertheless, both materials are having similar bandgap energy of (0.67 eV for Ge) and (0.74 eV for InGaAs), which consider efficient NB semiconductor for TPV application.

Several studies have highlighted the performance of Ge and InGaAs cells under various illumination concentrations [20]–[22], blackbody temperatures [23]–[25] and gap distances [15]. Typically, the TPV cells are employed under a wide range of spectral irradiances and operate at various illumination intensities. The intensity of the beam depends on the radiator temperature and gap distance (GD) between the radiator and TPV cells. Different illumination intensity may influence the amount of photo-generated current density and has a significant impact on the cell performance parameters, such as open-circuit voltage (V_{oc}), fill factor (FF) and cell conversion efficiency (η) [25], [26]. To date, studies on the effect of TPV illumination intensity on NB semiconductor devices are done at limited radiation temperatures and illumination intensities. Moreover, there is a lack in the understanding of the parameters governing FF, series resistance (R_s) and shunt resistance (R_{sh}) under TPV illumination intensity variations. A comparative study of indirect and direct bandgap TPV cells under various TPV spectral irradiances is yet to be conducted.

To understand the effect of illumination intensity on the FF, η, R_s and R_{sh} of direct and indirect bandgap semiconductor structures, further characterization work is needed. Modeling high-efficiency TPV cells under different TPV spectrum irradiances is therefore scientifically and commercially essential. In this regard, this study investigates the performance of indirect (Ge) and direct (InGaAs) NB semiconductor materials as a function of TPV illumination intensity. The performance of both cells at varying illumination intensities with the minimum electrical/optical losses is also investigated. Based on the results, the performance parameters such as short-circuit current density (J_{sc}), V_{oc}, FF, η, R_s and R_{sh} are broadly analyzed and studied.

II. PERFORMANCE/RELATED STUDIES ON GE AND INGAAS TPV CELLS

Ge has a cheaper material cost relative to other TPV cell materials [15], [27]. The synthesis cost of Ge TPV cell can be further reduced with hydrogenated amorphous silicon (a-Si:H) over flexible monocrystalline/c-Ge [28], [29]. Despite the high toxicity of precursors used in the growth of Ge and InGaAs cells by metal-organic vapour phase epitaxy (MOVPE), a growth advancement in Ge cell was achieved with the use of less toxic precursor isobutylgermane (IBuGe) as compared to germane (GeH_4) [30], [31]. Nevertheless, Ge has a few challenges, such as low V_{oc} [32] and high-temperature coefficient [27]. Therefore, the application of Ge cell in TPV system requires an efficient cooling system to prevent further reduction of cell efficiency.

On the other hand, InGaAs can be regarded as an efficient III-V semiconductor material for TPV applications. The advancement of InGaAs in MIM lattice-matched to InP substrate, high crystal quality, and excellent photoelectric properties make InGaAs a suitable candidate for large TPV panel [19]. Ge and InGaAs cells are commonly implemented in a multi-junction cell [33] and tandem cell [34] to extend the power harvesting up to near-infrared wavelengths (1800 nm), enhancing the cell conversion efficiency. Table 1 reviews the performances of Ge and InGaAs cells under solar and TPV illumination conditions. The variation in cells performance is influenced by factors such as photons absorption, generation, diffusion, electron/hole separation and collection. Besides, the generation, recombination and collection of electron/hole are governed by a complex interplay between the effect of active layer thickness, charge transport, recombination rate and more importantly, illumination intensity [35].

III. EXPERIMENTAL DETAILS

A. MODEL VALIDATION OF GE AND INGAAS CELLS

The epitaxial of Ge and InGaAs TPV cells in this study are shown in Figure 1(a) and 1(b), respectively. Silvaco TCAD tool was used to model the structures and to solve for the models' performance parameters. The simulation models of Ge and InGaAs were based on the structures reported by Kim *et al.* [37] and Sodabanlu *et al.* [17], respectively. For Ge TPV cell structure, the thickness (doping concentration) of the n-type Ge emitter layer was 0.05 μm (2×10^{19} cm^{-3}), whereas for the p-type Ge base layer was designed at 5 μm (2×10^{18} cm^{-3}). A 0.03 μm thick n-type window layer with 2×10^{19} cm^{-3} doping concentration of indium gallium phosphide (InGaP) was designed on top of the Ge emitter layer as an in-situ epitaxial surface passivation layer. Besides, a highly-doped ($>5 \times 10^{18}$ cm^{-3}) n-type gallium arsenide (GaAs) layer was employed with a thickness of 0.3 nm as a capping layer for ohmic contact formation. AuGe/Ni/Au and Ti/Pt/Au metallization structures were used as n- and p-type ohmic contact metals with a thickness of 0.15 μm. Finally, MgF_2/ZnS anti-reflection coating (ARC) is included to reduce optical loss [37].

TABLE 1. Ge and InGaAs TPV cells performance at various testing conditions.

Ref	Material	Str	V_{oc} (V)	J_{sc} (mA/cm^2)	FF (%)	η (%)	Test condition	Highlight
[20]	Ge	n-p	[a]0.32-0.38	n/a	[a]73.38-76.9	[a]9.65-11.8	2000 K (3.66-36.6 W/cm^2)	The J_{sc} increases linearly, while V_{oc} increases logarithmically with higher light intensity. The FF increases under the effect of both V_{oc} and V_m.
[28]		p-n	[a]0.05-0.27	n/a	n/a	n/a	0.001-1.5 suns	Suns–V_{oc} measurements were conducted using a WCT-120 Suns–V_{oc} Tester. The R_{sh} is sufficiently high such that the V_{oc} increases with suns.
[32]		p-n	n/a	n/a	n/a	[b]6.5-8.5 [b]7.5-9.8	AM1.5(40-500 suns) 1600-2000 K	Illustrate the performance of the Ge cell under different sunlight concentration. Furthermore, Fresnel lens used to heat up tungsten emitter.
[16]		n-p	0.205 & 0.282	42.1& 799.3	61.8 & 60	5.34 & 5.3	AM1.5(1 & 20 suns)	Test the proposed cell under high illumination densities. FF dropped with 20 sun concentration since contact pattern was designed for only 10 suns.
[25]	InGaAs	n/a	[a]0.11-0.225	[a]0.02 – 0.5	[a]43-58	[a]9.2 – 16.4	873-1323 K	The change in the radiation spectrum has a significant effect on current mechanisms, and it dominates the minority transport process.
[23]		n-p	[a]0.275-0.44	[b]1-600	n/a	[b]0.5-18	1000-6000 K (0.1 & 1 W/cm^2)	For blackbody temperature < 4000 K, InGaAs cell produces better η as compared to 1-1.2 eV cells. This is due to the shift of spectrum emission peak to IRs.
[36]		n-p-n	[a]2.8-5	[a]0.01-1.5	[a]67-73	n/a	Halogen tungsten 1920 K	Characterization of ten connected InGaAs cells as a function of light intensity. The V_{oc} increases logarithmically with increasing J_{sc}.

[a] parameter increases with intensity & [b] variable increases/decreases with intensity

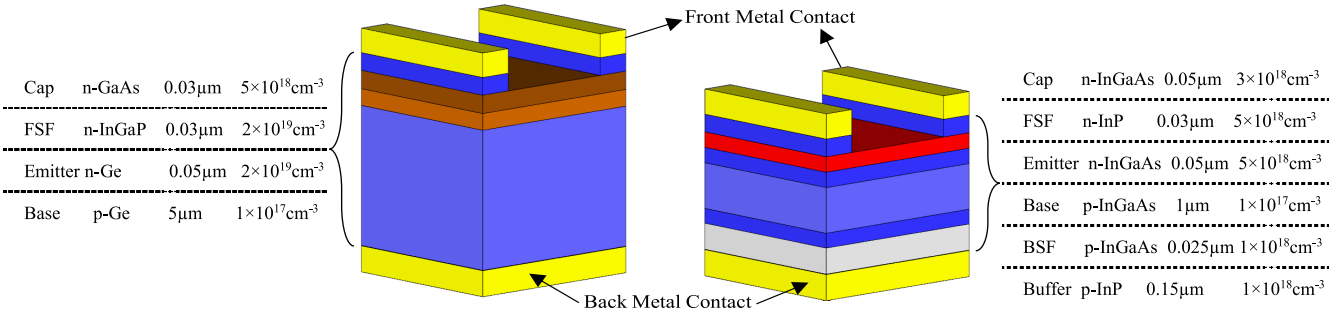

FIGURE 1. Baseline schematic cross-section of the epitaxial (a) Ge structure [37] and (b) InGaAs structure [17].

For InGaAs TPV cell structure, the thickness (doping concentration) of the n-type InGaAs emitter layer was structured to 0.05 μm (5×10^{18} cm^{-3}), whereas the p-type InGaAs base layer was set at 1 μm (1×10^{17} cm^{-3}). Similar to Ge structure, a 0.03 μm thick n-type InP window layer with 5×10^{18} cm^{-3} doping concentration was used. The window layer prevents the high surface recombination velocity and eliminates the front surface dangling bonds. In addition, a p-type InGaAs back surface field (BSF) and p-type InP buffer layers were incorporated in the structure with thicknesses (doping concentrations) of 0.025 μm (1×10^{18} cm^{-3}) and 0.15 μm (1×10^{18} cm^{-3}), respectively. These layers were used to improve the collection of photo-generated carriers at the long-wavelength [38]. As for the capping layer, a highly doped (3×10^{18} cm^{-3}) n-type InGaAs layer with a thickness of 0.05 nm was designed. AuZn and AuGe metal electrodes with a thickness of 0.15 μm were used for ohmic contact with p-InP substrates and n- InGaAs contact layers, respectively.

The material parameters and models of both TPV cells were carefully designed to match the actual cell design and experimental testing condition. Physical models such as radiative (band-to-band), non-radiative Shockley–Read–Hall (SRH), Auger recombination, and concentration-dependent minority carrier model of lifetime and mobility are defined for 300 K cell temperature. The material parameters were adjusted and optimized based on the reported material parameters of Ge, GaAs, InP, InGaAs and InGaP [18], [33], [39]. The current density-voltage (JV) characteristics of the Ge and InGaAs cells were simulated and presented in Figure 2(a) and 2(b), respectively. Figure 2 shows a close agreement between the simulation model and the reported experimental data for both cells with less than 6.3% of percentage error. In particular, a percentage error of 4.37% and 0.62% were achieved for η of respective Ge and InGaAs cells, hence validates the Ge and InGaAs cells.

B. STUDY THE GE AND INGAAS TPV CELLS UNDER DIFFERENT SPECTRAL IRRADIANCES

The validated Ge and InGaAs models were modified with the same ohmic metal grid coverage of 7% and without ARC, for a fair comparison. As aforementioned, the TPV cell operates under various spectral irradiance of blackbody temperatures ($\leq$2000 K) with different GDs, as illustrated in Figure 3. Based on the inverse square law, the amount of power transferred from emitter to cell significantly decreases with a longer GD [40]. Since it is impractical to manipulate GD in the Silvaco TCAD tools, the beam intensities will be manipulated in this study. The beam intensities have a direct relation with GDs where the higher the intensity, the closer GD between the radiator and TPV cells, and vice versa.

In this work, the characterization of Ge and InGaAs TPV cells performance under various blackbody temperatures with different illumination intensities was performed. The illumination intensities of both cells were decreased from 100% to

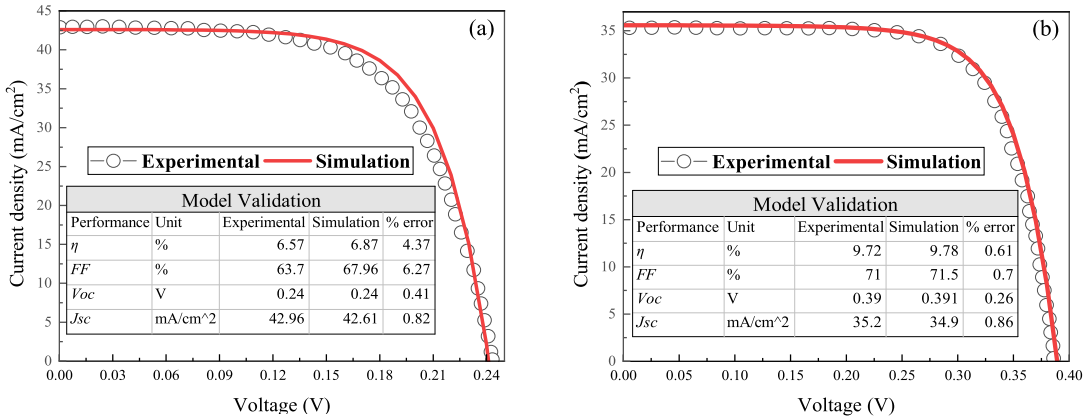

FIGURE 2. JV curve model validation at AM1.5 illumination condition for (a) the Ge cell [37] and (b) the InGaAs TPV cell [17].

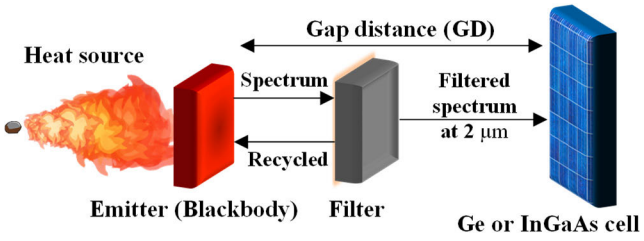

FIGURE 3. The schematic diagram of the TPV system.

10% with an interval of 10%. Similar illumination steps were reported for blackbody temperatures from 800 to 2000 K. The cell temperature was maintained at 300 K, assuming an effective cooling system was deployed [66]. Three main factors influence the efficiency of the Ge and InGaAs cells that are optical losses due to the front surface reflection, insufficient absorber thickness, as well as, the R_s and R_{sh}. The R_s of both Ge and InGaAs cells can be minimized with the use of ohmic metal contact. Therefore, an additional analysis was conducted to characterize the performance of both Ge and InGaAs cells at different radiation temperatures with minimum optical losses. The optical losses were minimized with the use of ARC and optimum thickness for the absorber layer. For the Ge cell, the absorber (base layer) thickness was varied from 1 to 170 μm while the InGaAs base thickness was varied from 1 to 20 μm. The optimum thickness was selected based on the optimum efficiency of the cells under TPV testing conditions.

In addition, a 2 μm low pass optical filter was employed in the simulation following the spectral irradiance of the reported TPV system [41], [42]. Fourspring *et al.* [43] illustrated the use of an optical interference filter generates high spectral efficiency for wavelength lower than 2 μm. The filter allows convertible photons to pass through and maximize the photon absorption and the conversion efficiency of the TPV cell [11], [44]. With the application of a low pass optical filter, the illumination intensities varied between 0.0046 and 43.6 W/cm^2 for blackbody temperatures from 800 to 2000 K.

IV. RESULTS AND DISCUSSIONS

A. THE JV CURVES OF THE GE AND INGAAS TPV CELLS UNDER DIFFERENT ILLUMINATION INTENSITIES

Figures 4(a) and 4(b) show the *JV* characteristics of the Ge and InGaAs cells under 1400 K blackbody temperature with different illumination intensities. It is worth mentioning that a similar trend is reported for other blackbody temperatures. For Ge cell, as the beam intensity increased from 10% to 100%, both J_{sc} and V_{oc} increased from 105 to 1050 mA/cm^2 and 0.27 to 0.33 V, respectively. A similar trend is reported for the InGaAs cell with slightly higher J_{sc} and V_{oc}. Besides, the trend found in this study is in a good agreement with a work published by Su *et al.* [22] for InGaAs under concentration ratio of ~1−27 sun. It was reported that J_{sc} increased rapidly with the increase of illumination intensity while V_{oc} increased gradually. The effect of illumination intensity on J_{sc} is expressed in Equation (1).

$$J_{sc} = \int_0^{\lambda(E_g)} \Phi(\lambda) EQE(\lambda) d \tag{1}$$

where Φ is the illumination intensity, *EQE* is the external quantum efficiency, and d is the device thickness. Since *EQE* and d were constant when the physical, electrical, and optical parameters of the Ge and InGaAs cells remain constant throughout the simulation, the J_{sc} linearly increased with the illumination intensity. On the other hand, the relationship between V_{oc} and I_{sc} can be described by diode equation after setting the net current of the cell to zero.

$$V_{oc} = \frac{nk_BT}{q} \ln\left(\frac{I_{sc}}{I_o} + 1\right) \tag{2}$$

where n is the ideality factor, k_B is the Boltzmann constant, T is the cell temperature, q is the charge, and I_o is the dark current. From Equation (2), it can be seen that the linear increase of I_{sc} will proportionally increase the V_{oc} in a logarithmic manner. In terms of the ratio of absorption to emission, which represents the light generated current density to the reverse saturation current (I_{sc}/I_o) in Equation (2), the V_{oc} increases logarithmically either by increasing I_{sc} or

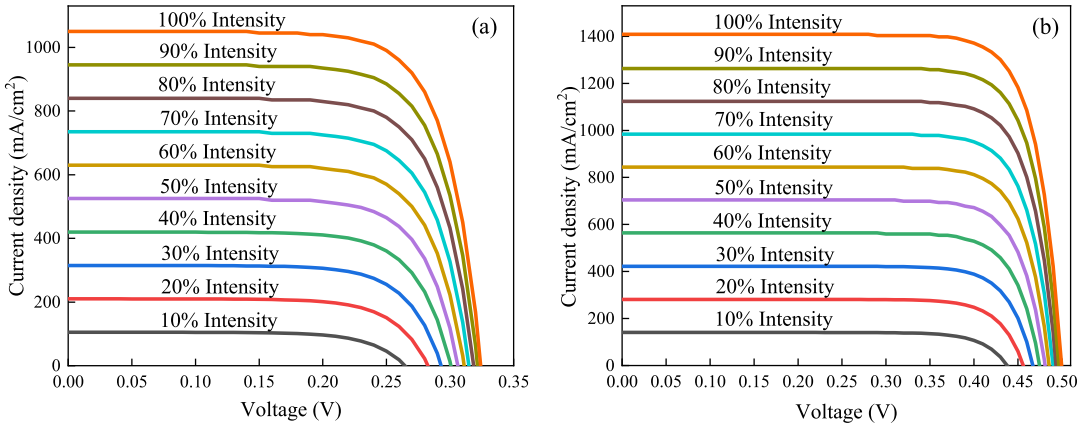

FIGURE 4. JV curves of 1400 K blackbody temperature under various intensities for (a) the Ge TPV cell and (b) the InGaAs TPV cell.

TABLE 2. The performance parameters of Ge TPV Cell under 10% of the beam intensity.

Blackbody temperature		800 K	1000 K	1200 K	1400 K	1600 K	1800 K	2000 K
P_{in} (W/cm^2)		0.0046	0.0378	0.1648	0.4961	1.1812	2.4007	4.3597
Performance	J_{sc} (mA/cm^2)	0.40	4.89	28.30	105.00	291.00	661.00	1300.00
	V_{oc} (V)	0.12	0.19	0.23	0.27	0.29	0.31	0.33
	FF (%)	53.20	62.70	67.10	69.90	71.60	72.90	73.70
	η (%)	0.57	1.50	2.66	3.91	5.13	6.27	7.28
	R_s (Ω cm^2)	86.77	6.98	1.16	0.31	0.11	0.05	0.02
	R_{sh} (kΩ cm^2)	3.42	3.24	2.57	1.55	0.80	0.43	0.22

decreasing I_o [45]. Since the TPV cells usually operate at high illumination intensity [22], [26], the I_{sc} is always significantly larger than I_o. Therefore, increasing the illumination intensity will eventually increase V_{oc} performance.

Another explanation for the increment of V_{oc} can be realized from the band diagram. The increase in illumination intensity rises the excited carrier concentrations and their redistribution. This triggers the splitting of the equilibrium Fermi level into the minority carrier electron and hole quasi-Fermi level. Higher illumination will therefore cause a larger quasi-Fermi level separation. Since the cell voltage is derived from the quasi-Fermi level separation, increasing the light concentration will increase the V_{oc}. Moreover, this increment was reported to be the main contributor to a higher η in work done by Algora and Stolle [46].

B. EFFECT OF DIFFERENT SPECTRAL IRRADIANCES ON THE PERFORMANCE OF GE AND INGAAS TPV CELLS

Different illumination intensities would give a significant impact on the cell performance parameters such as J_{sc}, V_{oc}, FF, η, R_s, and R_{sh} [26]. Tables 2 and 3 present the performance of Ge and InGaAs cells, respectively, for blackbody temperatures from 800 to 2000 K with a beam intensity of 10%. For all performance parameters, it can be seen that the InGaAs cell performs better than the Ge cell. The J_{sc} of InGaAs TPV cell is higher for all radiation temperatures, which indicates the high absorption of the infrared photons. On the contrary, the V_{oc} of Ge cell is significantly lower due to their high reverse saturation current [47]. The V_{oc} is influenced by the dark current densities, J_{01} and J_{02}, where J_{01} represents the dark current due to surface and bulk recombination losses and J_{02} is related to recombination due to traps in the SCR [28].

The η of the Ge and InGaAs cells increased from 0.57 to 7.28% and 3.18 to 14.30%, respectively, as the input power density (P_{in}) increased from 0.0046 to 4.3498 W/cm^2. It can be observed that the improvement in InGaAs cell is more significant than that of the Ge cell. The efficiency's increment of both cells is governed by the FF, as shown in Equation (3).

$$\eta = \frac{P_{out}}{P_{in}} = \frac{V_{oc} I_{sc} FF}{P_{in}} \tag{3}$$

The FF of Ge and InGaAs cells increased from 53.20 to 72.90% and 69.90 to 79.90%, respectively, as the P_{in} increased. Although the improvement of FF for Ge cell is better than that of the InGaAs cell, InGaAs has higher FF values with a peak FF of 79.90% at 2000 K blackbody temperature. The figure of merit for TPV performance is presented by FF, which is defined as the ratio of the cell's maximum power (P_{mp}) to the $I_{sc}V_{oc}$ product, as shown in Equation (4):

$$FF = \frac{V_{mp} I_{mp}}{V_{oc} I_{sc}} \tag{4}$$

where V_{mp} is the maximum voltage, and I_{mp} is the maximum current of actual operating condition taking R_s and R_{sh} into consideration for the cell performance [48]. While the R_s is contributed by the resistance of semiconductor layers, metal contacts, interface between the semiconductor layers and

TABLE 3. The performance parameters of InGaAs TPV Cell under 10% of the beam intensity.

Blackbody temperature		800 K	1000 K	1200 K	1400 K	1600 K	1800 K	2000 K
P_{in} (W/cm^2)		0.0046	0.0378	0.1648	0.4961	1.1812	2.4007	4.3597
Performance	J_{sc} (mA/cm^2)	0.71	7.72	40.80	141.00	370.00	809.00	1550.00
	V_{oc} (V)	0.30	0.36	0.41	0.44	0.46	0.48	0.50
	FF (%)	69.90	74.40	76.60	77.90	78.90	79.50	79.90
	η (%)	3.18	5.47	7.67	9.68	11.50	13.00	14.30
	R_s (Ω cm^2)	1492.92	112.90	23.44	6.31	2.13	0.96	0.52
	R_{sh} (kΩ cm^2)	99.60	79.70	37.20	14.00	5.58	2.79	1.40

interface between the semiconductor layer and metal contact, the R_{sh} is influenced by the crystal defects and precipitates of foreign impurities [14]. Correspondingly, R_{sh} represents the leakage across the junction and around the edge of the cell. It describes the crystal defects and precipitates of foreign impurities [14]. The enhancement of FF attributes to a low R_s ($R_s \sim 0$) and a high R_{sh}($R_{sh} \sim \infty$). This relationship is expressed as follow [48]:

$$FF(R_s, R_{sh}) \approx FF(0, \infty) \times (1 - \frac{J_{sc} - R_s}{V_{oc}} - \frac{V_{oc}}{J_{sc} - R_{sh}}) \quad (5)$$

The relationship of R_s and R_{sh} as a function of PV intensity was highlighted for Si, GaAs and CdTe cells [26], [49]–[51]. However, the relationship of R_s and R_{sh} as a function of TPV intensities is yet to be reported. There are several methods which can be employed to extract the R_s and R_{sh}. Curve fitting, which is the analytical method or numerical method, requires the dark or illuminated IV characteristics [52]–[55]. In this study, the R_s and R_{sh} were calculated using the JV characteristics curve. The R_{sh} is the inverse of the slope $\{(dJ/dV)^{-1}\}$ under short circuit condition when $V = 0$ and $J = -J_{sc}$. On the other hand, the following equation was used to extract R_s [50].

$$R_s = R_{oc} - \frac{(V_{mp} + R_{oc}J_{mp} - V_{oc})}{J_{mp} + \{\ln(J_{sc} - J_{mp}) - \ln(J_{sc})\} * J_{sc}} \quad (6)$$

where R_{oc} is the inverse of the slop $\{(dJ/dV)^{-1}\}$ under open circuit condition when $V = V_{oc}$ and $J = 0$. Under dark condition, the R_s and R_{sh} of the Ge (InGaAs) cells were 5.32 (112.55) Ω cm^2 and 3.43 (105.23) kΩ cm^2, respectively. As the power density increased, R_s of the Ge cell (InGaAs cell) decreased from 86.77 to 0.02 Ω cm^2 (1492.92 to 0.52 Ω cm^2) while R_{sh} of the Ge cell (InGaAs cell) decreased from 3.43 Ω cm^2 to 0.22 Ω cm^2 (99.6 to 1.40 Ω cm^2). It can be observed that the reduction of R_s with higher blackbody temperature play a crucial role in improving the FF for both cells. Furthermore, higher R_{sh} value of InGaAs cell demonstrates its advantage of having a low leakage current and good crystal quality for TPV illumination [56].

Further characterization works were then performed to understand the influence of different spectral irradiances on the performance of the Ge and InGaAs cells. Spectral irradiances herein refer to the manipulation of blackbody temperatures from 800 to 2000 K with beam intensities between 10 to 100%. The output performance parameters (J_{sc}, V_{oc}, FF, R_s, R_{sh} and η) of the Ge and InGaAs cells were normalized to the 10% of the beam intensity and presented as normalized J_{sc}, normalized V_{oc}, normalized FF, normalized R_s, and normalized R_{sh} and normalized η.

Figures 5(a) and 5(b) illustrate the normalized J_{sc} as a function of different spectral irradiances. It is clear that the normalized J_{sc} curves under different temperatures for both Ge and InGaAs cells have similar trend, demonstrating that the generation and recombination increases by similar rate with the increment of beam intensity. Meanwhile, Figures 5(c) and 5(d) demonstrate the logarithmical relationship between intensity and the normalized V_{oc}. Overall, under different spectral irradiances, the V_{oc} of InGaAs cell was higher than that of the Ge cell. However, the Ge cell reported higher growth in the normalized V_{oc} as compared to the InGaAs cell. This is associated with the increment of the generation/recombination ratio in the indirect bandgap cells as the beam intensities increased. In indirect bandgap semiconductor materials, the trap assisted recombination (RSH recombination) is usually dominant. This recombination mechanism involves the trapping of an electron or holes followed by re-emission into the valance or conduction band [37], [57].

The normalized fill factor exhibits a different trend of performance as compared to normalized J_{sc} and normalized V_{oc}. Figures 6(a) and 6(b) show the normalized FF of the Ge and InGaAs cells as a function of different spectral irradiances. A continuous increment in the normalized FF of the Ge cell was reported at different spectral irradiances. While at temperature $\geq$1800 K, the normalized FF of the InGaAs cell starts to saturate when the beam intensity exceeds 40%, this is mainly due to the effect of the R_s and R_{sh} as shown in Figures 6(c)-6(f). Researchers have investigated the performance of FF under various sun concentration and blackbody temperatures [22], [50], [58]. It was reported that FF increased with higher blackbody temperature due to the increment of V_{oc} incorporated with high light absorption [25]. Furthermore, an increase in the beam intensity will decrease the R_s and enhance FF [22]. However, a significant increment in the beam power density will decrease the FF under the effect of both R_s and R_{sh} [50]. The investigation of Si PV cell

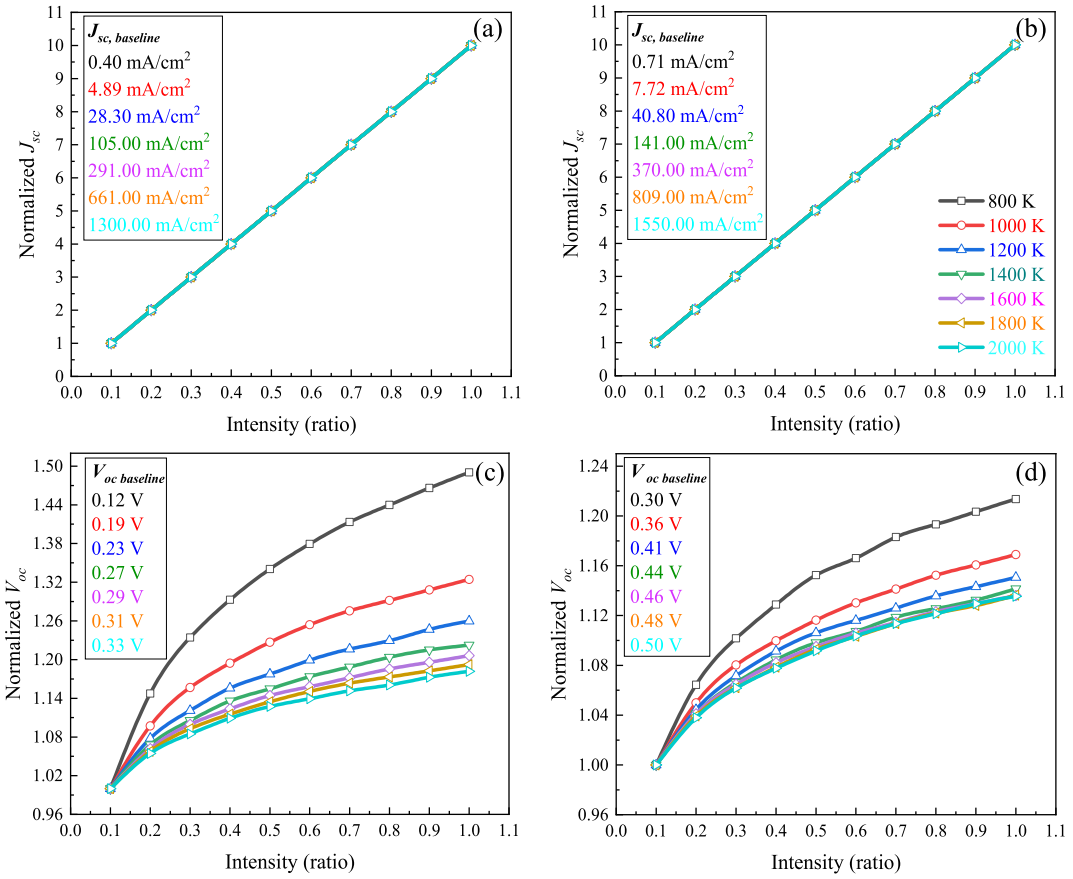

FIGURE 5. Normalized current density under various spectral irradiance for (a) Ge TPV cell and (b) InGaAs TPV cell; and normalized open-circuit voltage under different spectral irradiance for (c) Ge TPV cell and (d) InGaAs TPV cell. The $J_{sc\,baseline}$ and $V_{oc\,baseline}$ represent the J_{sc} and V_{oc} at 10% of the beam intensity, and color indicates different radiation temperatures.

had shown that *FF* increased with beam intensity from 20 to 50 mW/cm^2 [51], and decreased when illumination irradiance was higher than 200 mW/cm^2 [50]. The enhancement of the *FF* can be obtained after optimizing the metal contacts and cell configuration for high intensities.

As aforementioned, the variation in *FF* is related to both R_s and R_{sh} of the cell. Figures 6(c)-6(f) show the normalized R_s and the normalized R_{sh} of the Ge and InGaAs cells as a function of different spectral irradiances. It is observed that the R_s and the R_{sh} of both Ge and InGaAs cells decrease with higher illumination intensities. A reasonable justification for the decline in R_s is due to the increase in the semiconductor layers conductivity with high illumination intensity as reported for the Si, GaAs and CdTe cells [26], [50], [51]. Since the metal contacts of the cells were designed to be ohmic, the change of R_s with increasing illumination intensity was dominated by the semiconductor layers and interface/semiconductor junction. The increase in *FF* is due to the increase in the conductivity of the semiconductor layers, as photogenerated carriers increased. However, when the current flow in the cells is significantly high, the R_s which is dominated by the semiconductor conductivity reduces to very low value and then it saturates. After the saturation of the R_s, the electrical losses I^2R_s become significant. Minimizing the I^2R_s losses associated with high current requires the reduction of R_s. At a given point of intensity, the effects of the I^2R_s losses become apparent, and *FF* starts to decline [21]. Cell performance was usually presented as a function of current density due to the high impact of R_s at higher illumination intensity [58], [59]. For example, the efficiency of the Ge started to reduce when J_{sc} was higher than 5 A/cm^2 [32]. Moreover, high illumination increases the carrier generation, resulting in bimolecular recombination which degrades cell resistance [35].

On the other hand, the normalized R_{sh} of Ge and InGaAs cells decrease with higher intensity due to the increase in the carriers' recombination rate. The recombination rate is proportional to the generation rate. The rate of decreasing normalized R_{sh} of the Ge cell is slightly lower than that of InGaAs cell. An indirect bandgap semiconductor material has low recombination rate since it requires the change in the energy and the moment to complete the recombination process. Furthermore, an indirect bandgap semiconductor material such as Ge has higher trap defects in the SCR which act as a sink for photo-generated minority charge carriers [49]. These traps begin to be filled when the intensity increases from 0.0046 to 0.0092 W/cm^2. The further increment in

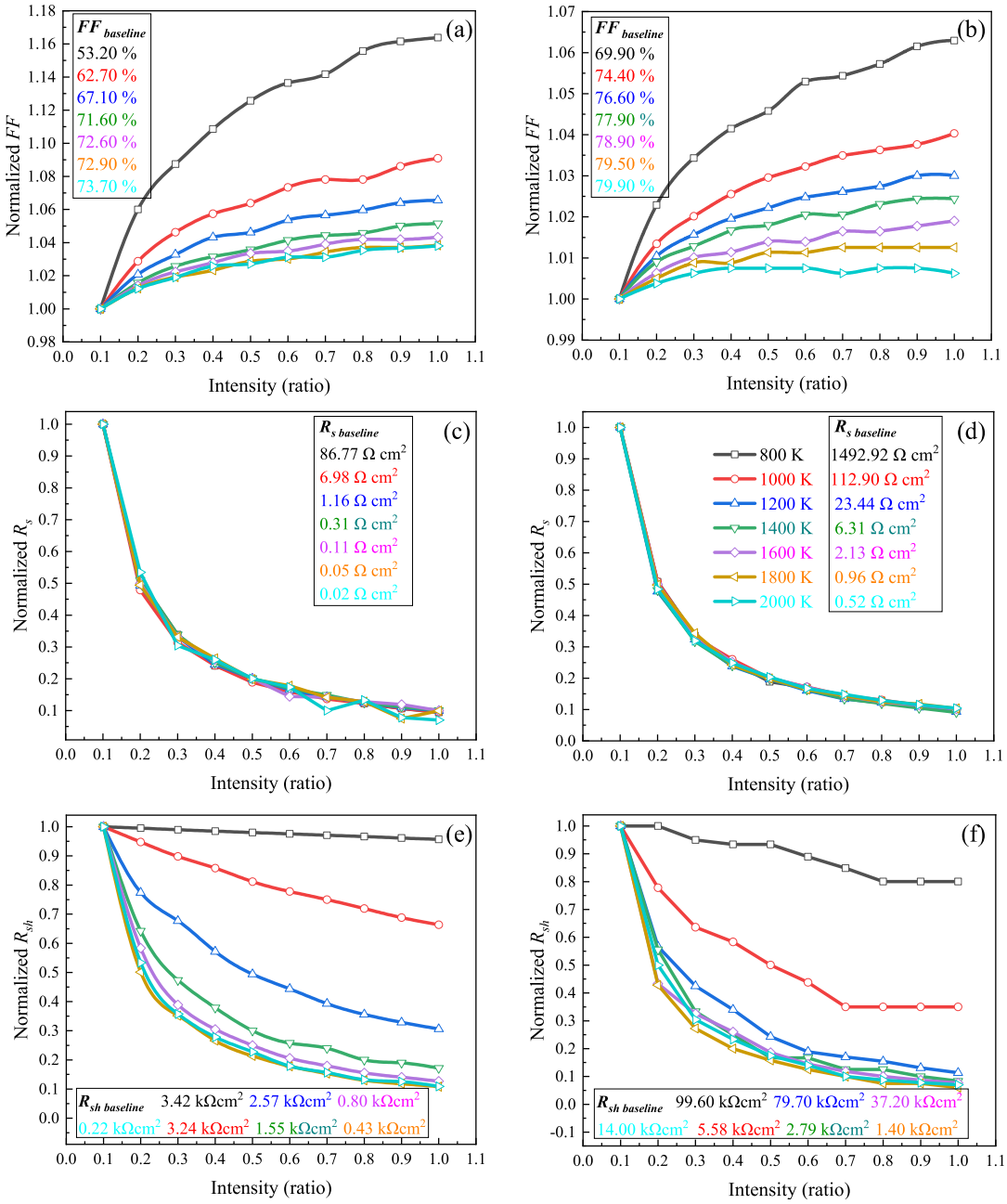

FIGURE 6. Normalized fill factor under various spectral irradiance for (a) Ge TPV cell and (b) InGaAs TPV cell; Normalized series resistance under different spectral irradiance for (c) Ge TPV cell and (d) InGaAs TPV cell; and normalized shunt resistance under different spectral irradiance for (e) Ge TPV cell and (f) InGaAs TPV cell. TPV cell. The $FF_{baseline}$, $R_{s\,baseline}$ and $R_{sh\,baseline}$ represent the FF, R_S and R_{sh} at 10% of the beam intensity, and color indicates different radiation temperatures.

the intensity (>0.0092 W/cm^2) increases the shunt current, resulting in lower R_{sh}.

Next, the effect of increasing illumination intensity on the Ge and InGaAs cells normalized efficiency are presented in Figure 7. While the J_{sc} increased proportionally with the illumination intensity, the increment of η was governed by the rise of the V_{oc} and FF performance outputs. Figures 7(a) and 7(b) show that normalized η increased with higher illumination intensity. Notably, for InGaAs cell that operates under blackbody temperatures ≥1800 K, the normalized η starts to saturate at illumination intensities of greater than 40%. This is attributed to the decline of FF and the gradual increase of V_{oc} under high spectrum irradiances. In addition, the Ge cell obtained higher normalized η increment as the beam intensity increased from 10 to 100%. This finding indicates that the efficiency enhancement of the indirect bandgap TPV cell is better than the direct bandgap TPV cell when operates under high illumination intensities.

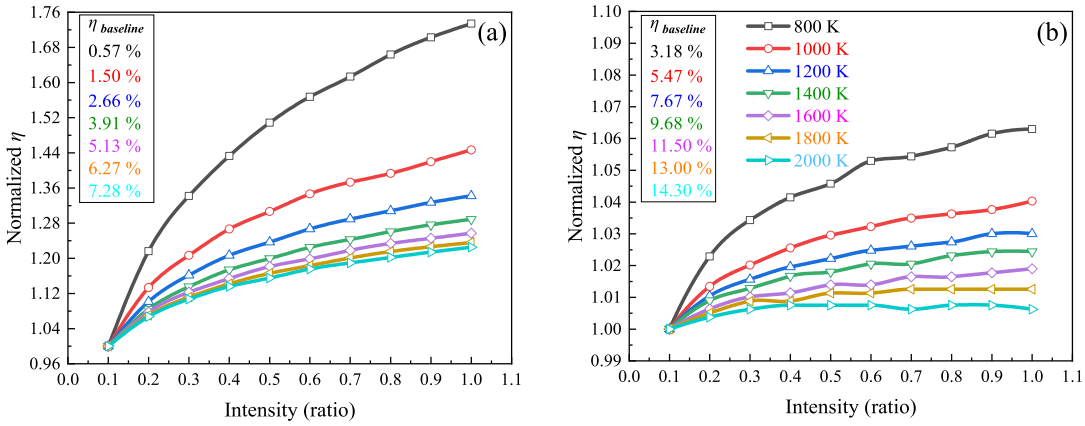

FIGURE 7. Normalized efficiency under various spectral irradiance for (a) and Ge TPV cell and (b) InGaAs TPV cell. The η_{baseline} represents the η at 10% of the beam intensity, and color indicates different radiation temperatures.

C. THE GE AND INGAAS CELLS PERFORMANCE UNDER VARIOUS RADIATION'S TEMPERATURES BEFORE/AFTER IMPROVING THE OPTICAL LOSSES

The cells were investigated under different radiation temperatures before and after optimizing the TPV cells for minimum optical losses. Since the paper's main focus is to study the intensity effect, optimization was only conducted for the base layer thicknesses, which is the main contributing factor [60], and the radiation temperature was at 1800 K. Furthermore, effective ARC such as MgF_2/ZnS for the Ge cell and MgF_2/ZnSe for InGaAs cell are employed to reduce the optical reflection losses at the surface of cells [37], [61]. The efficiency of Ge or InGaAs cells increases after the use of ARC due to the reduction of the incident light reflects at the front surface of the cell. ARC accounted for about 40% of the efficiency improvement of the cells. For example, at 1800 K radiation temperature, the efficiency of the non-optimized Ge (InGaAs) cell increased from 5.68 (14.34) to 8.11% (20.23%), solely due to the application of ARC. A similar observation has been reported by Shemelya *et al.* [62] and Sharma *et al.* [63], where an efficiency improvement between 30 and 50% was achieved with the utilization of ARC. Additionally, the optical losses due to low absorption in the structure were reduced by optimizing the thickness of the absorber. As shown in Figure 8, the thicknesses of Ge (InGaAs) base layers were varied from 1 to 170 μm (1 to 30 μm) while the rest of the layers were maintained at the same values.

It was found that maximum conversion efficiencies can be obtained with an optimum absorber thickness (base layer) of 150 μm and 7 μm for Ge and the InGaAs cells, respectively. The increment of absorber thickness enhances the harvesting of band edge radiation for both cells. Nevertheless, InGaAs requires a thinner absorber layer as compared to Ge cell due to the direct bandgap properties [64]. Figure 8 presents the efficiency of the Ge and InGaAs cells before and after minimizing the optical losses for blackbody temperatures from 800 to 2000 K.

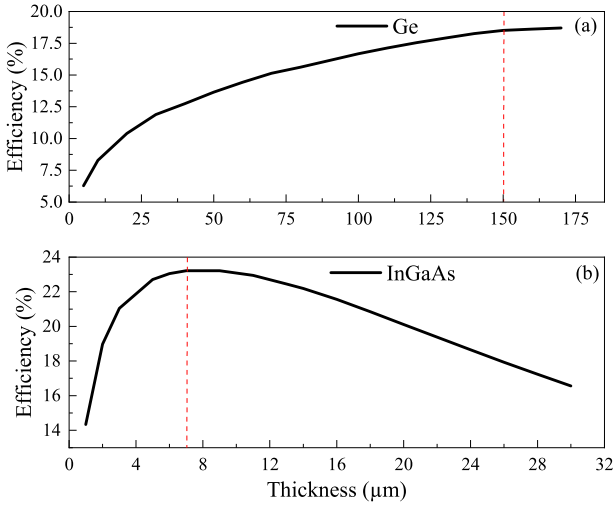

FIGURE 8. The TPV cell efficiency versus the base layer thickness for (a) Ge TPV cell and (b) InGaAs TPV cell.

It is observed that as the blackbody temperature increases, the η of both Ge and InGaAs cells were gradually increased. This behavior is related to the increase in the total spectral energy density, as well as the number of radiation photons which are below the cutoff wavelength of the TPV cells when the temperature of the radiation increases. For example, as the radiation temperature increases from 800 to 2000 K, the energy density increases from 0.0046 W/cm^2 to 4.3597 W/cm^2. Furthermore, majority of the photons shift towards the convertible range of Ge and InGaAs TPV cells, which are from 3.63 to 1.45 μm.

As shown in Figure 9, Ge cell has higher efficiencies in comparison to InGaAs cell when the radiation temperature was <1000 K. This is because Ge cell has a cutoff wavelength of 1.8 μm which is slightly longer than the 1.6 μm cutoff of InGaAs cell. The ability to harvest longer wavelength of Ge combined with the high concentration of optical radiation at low source temperatures allows the Ge cell to produce higher cell efficiency. In addition, under radiation temperatures from 800 to 2000 K, Ge and InGaAs cells have an

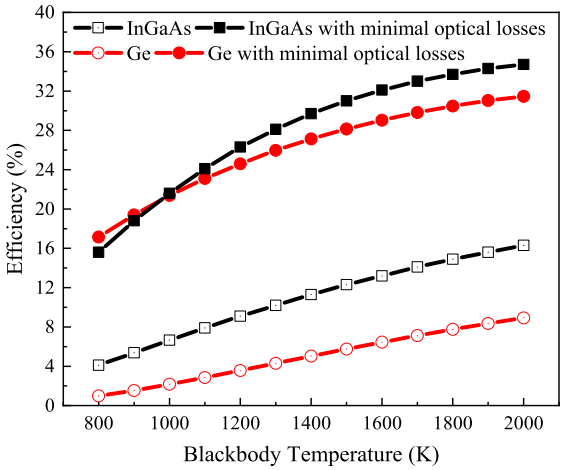

FIGURE 9. Ge and InGaAs TPV cells efficiency before/after improving the optical losses. Minimal optical losses represent the cells with optimum base thickness and ARC.

average efficiency of ∼4.34% and 8.45%, respectively. The average efficiency improved to 26.05% and 27.92% after minimizing the optical losses. In general, InGaAs TPV cell has higher efficiencies under various blackbody temperature. However, Ge cell can produce a comparable performance when both electrical losses and optical losses are minimized.

V. CONCLUSION

In summary, the validated Ge and InGaAs cells are studied under different TPV spectral irradiances. It was found that:

- The J_{sc} and normalized J_{sc} of both cells increase linearly with the increase of TPV beam intensity due to the rise of the photo-generated carriers within the absorber region.
- The V_{oc} and normalized V_{oc} increase logarithmically with the increase of TPV beam intensity. Furthermore, indirect bandgap (Ge cell) has higher normalized V_{oc} increment as compared to direct bandgap (InGaAs cell) due to the significant increment of the generation/recombination ratio.
- The *FF* and normalized *FF* continuously increase under high illumination intensity for both Ge and InGaAs cells. At temperatures ≥1800 K, the normalized *FF* of the InGaAs cell starts to saturate when the beam intensity exceeds 40%, which is mainly due to the effect of the R_s and R_{sh}.
- The normalized R_s of Ge and InGaAs cells decrease rapidly with increasing illumination intensity due to the increase in conductivity of the devices. R_s dominate the power losses (I^2R), and reducing it will enhance cell performance.
- The normalized R_{sh} of both Ge and InGaAs cells decrease rapidly with increasing illumination intensity. However, the reduction rate of normalized R_{sh} for Ge cell is lower than that of InGaAs cell. This is attributed to the lower recombination rate of indirect semiconductor since requires the change in the energy and the moment to complete the recombination process.
- The ohmic resistance between the semiconductor and the metal contacts are critical in designing high-performance TPV cells that are capable of operating at high illumination intensities. Further improvement in the performance of cells are observed with the use of ARC and thicker absorber. At 2000 K blackbody temperature, maximum cell efficiencies of 31.46% and 34.72% are reported for Ge and InGaAs TPV cells, respectively. In general, under various TPV spectral irradiances, Ge cell with optimum absorber layer is able to produce comparable output performance compared to InGaAs, but at the expense of having a very thick absorber layer.

The results of this work contribute to the development of high-performance TPV system by demonstrating that high-efficiency TPV cells could be achieved through comprehensive considerations of the design structures and spectral irradiances.

REFERENCES

[1] X. Wang, R. Liang, P. Fisher, W. Chan, and J. Xu, "Radioisotope thermophotovoltaic generator design methods and performance estimates for space missions," *J. Propuls. Power*, vol. 36, no. 4, pp. 593–603, Jul. 2020.
[2] L. M. Fraas, "Thermophotovoltaics using infrared sensitive cells in low-cost solar electric power," in *Low-Cost Solar Electric Power*. Cham, Switzerland: Springer, 2014.
[3] M. Seal, S. Christ, G. Campbell, E. West, and L. Fraas, "Thermophotovoltaic generation of power for use in a series hybrid vehicle," *SAE Tech. Papers*, vol. 56, no. 11, pp. 8–55, Aug. 1997.
[4] A. Krier, M. Yin, A. R. J. Marshall, and S. E. Krier, "Low bandgap InAs-based thermophotovoltaic cells for heat-electricity conversion," *J. Electron. Mater.*, vol. 45, no. 6, pp. 2826–2830, Jun. 2016.
[5] A. Lenert, D. M. Bierman, Y. Nam, W. R. Chan, I. Celanović, M. Soljačić, and E. N. Wang, "A nanophotonic solar thermophotovoltaic device," *Nature Nanotechnol.*, vol. 9, no. 2, pp. 126–130, Feb. 2014.
[6] M. Elzouka and S. Ndao, "Towards a near-field concentrated solar thermophotovoltaic microsystem: Part I—Modeling," *Sol. Energy*, vol. 141, pp. 323–333, Jan. 2017.
[7] A. Datas, A. Ramos, A. Martí, C. del Cañizo, and A. Luque, "Ultra high temperature latent heat energy storage and thermophotovoltaic energy conversion," *Energy*, vol. 107, pp. 542–549, Jul. 2016.
[8] H. R. Seyf and A. Henry, "Thermophotovoltaics: A potential pathway to high efficiency concentrated solar power," *Energy Environ. Sci.*, vol. 9, no. 8, pp. 2654–2665, 2016.
[9] Z. Utlu and B. S. Önal, "Thermodynamic analysis of thermophotovoltaic systems used in waste heat recovery systems: An application," *Int. J. Low-Carbon Technol.*, vol. 13, no. 1, pp. 52–60, 2018.
[10] Z. Utlu, "Thermophotovoltaic applications in waste heat recovery systems: Example of GaSb cell," *Int. J. Low-Carbon Technol.*, vol. 15, no. 2, pp. 277–286, May 2020.
[11] S. Shan, Z. Zhou, and K. Cen, "An innovative integrated system concept between oxy-fuel thermo-photovoltaic device and a Brayton-Rankine combined cycle and its preliminary thermodynamic analysis," *Energy Convers. Manag.*, vol. 180, pp. 1139–1152, Jan. 2019.
[12] W. Emilin Suliza Wan Abdul Rashid, P. Jern Ker, M. Zaini Bin Jamaludin, M. Mohammed Ali Gamel, H. Jing Lee, and N. Bin Abd Rahman, "Recent development of thermophotovoltaic system for waste heat harvesting application and potential implementation in thermal power plant," *IEEE Access*, vol. 8, pp. 105156–105168, 2020.
[13] Z. Yang, W. Peng, T. Liao, Y. Zhao, G. Lin, and J. Chen, "An efficient method exploiting the waste heat from a direct carbon fuel cell by means of a thermophotovoltaic cell," *Energy Convers. Manag.*, vol. 149, pp. 424–431, Oct. 2017.
[14] M. A. Green, *Solar Cells: Operating Principles, Technology and System Applications*. Kensington, NSW, Australia: Univ. New South Wales, 1986.

[15] P. Sansoni, D. Fontani, F. Francini, D. Jafrancesco, G. Gabetta, M. Casale, R. Campesato, and G. Toniato, "Evaluation of elliptical optical cavity for a combustion thermophotovoltaic system," *Sol. Energy Mater. Sol. Cells*, vol. 171, pp. 282–292, Nov. 2017.

[16] J. van der Heide, N. E. Posthuma, G. Flamand, W. Geens, and J. Poortmans, "Cost-efficient thermophotovoltaic cells based on germanium substrates," *Sol. Energy Mater. Sol. Cells*, vol. 93, no. 10, pp. 1810–1816, Oct. 2009.

[17] H. Sodabanlu, K. Watanabe, M. Sugiyama, and Y. Nakano, "Growth of InGaAs(P) in planetary metalorganic vapor phase epitaxy reactor using tertiarybutylarsine and tertiarybutylphosphine for photovoltaic applications," *Jpn. J. Appl. Phys.*, vol. 57, no. 8S3, Aug. 2018, Art. no. 08RD09

[18] M. Levinshtein, S. Rumyantsev, and M. Shur, *Handbook Series on Semiconductor Parameters: Ternary And Quaternary III-V Compounds*, vol. 2. Singapore: World Scientific, 1996.

[19] R. S. Tuley, J. M. S. Orr, R. J. Nicholas, D. C. Rogers, P. J. Cannard, and S. Dosanjh, "Lattice-matched InGaAs on InP thermophovoltaic cells," *Semicond. Sci. Technol.*, vol. 28, no. 1, Jan. 2013, Art. no. 015013.

[20] M. M. A. Gamel, K. P. Jern, W. E. Rashid, L. K. Yau, and M. Z. Jamaludin, "The effect of illumination intensity on the performance of germanium based-thermophotovoltaic cell," in *Proc. IEEE Regional Symp. Micro Nanoelectronics (RSM)*, Aug. 2019, pp. 129–132.

[21] W. Guter, J. Schöne, S. P. Philipps, M. Steiner, G. Siefer, A. Wekkeli, E. Welser, E. Oliva, A. W. Bett, and F. Dimroth, "Current-matched triple-junction solar cell reaching 41.1% conversion efficiency under concentrated sunlight," *Appl. Phys. Lett.*, vol. 94, no. 22, pp. 94–97, 2009.

[22] N. Su, P. Fay, S. Sinharoy, D. Forbes, and D. Scheiman, "Characterization and modeling of InGaAs/InAsP thermophotovoltaic converters under high illumination intensities," *J. Appl. Phys.*, vol. 101, no. 6, Mar. 2007, Art. no. 064511.

[23] M. Emziane and R. J. Nicholas, "Optimization of InGaAs(P) photovoltaic cells lattice matched to InP," *J. Appl. Phys.*, vol. 101, no. 5, Mar. 2007, Art. no. 054503.

[24] M. Piness-Sommer, A. Braun, E. A. Katz, and J. M. Gordon, "Ultra-compact combustion-driven high-efficiency thermophotovoltaic generators," *Sol. Energy Mater. Sol. Cells*, vol. 157, pp. 953–959, Dec. 2016.

[25] M. Tan, L. Ji, Y. Wu, P. Dai, Q. Wang, K. Li, T. Yu, Y. Yu, S. Lu, and H. Yang, "Investigation of InGaAs thermophotovoltaic cells under blackbody radiation," *Appl. Phys. Exp.*, vol. 7, no. 9, Sep. 2014, Art. no. 096601.

[26] Q. Li, K. Shen, R. Yang, Y. Zhao, S. Lu, R. Wang, J. Dong, and D. Wang, "Comparative study of GaAs and CdTe solar cell performance under low-intensity light irradiance," *Sol. Energy*, vol. 157, pp. 216–226, Nov. 2017.

[27] O. V. Sulima, A. W. Bett, P. S. Dutta, M. G. Mauk, and R. L. Mueller, "GaSb-, InGaAsSb-, InGaSb-, InAsSbP- and ge-TPV cells with diffused emitters," in *Proc. Conf. Rec. 29th IEEE Photovoltaic Spec. Conf.*, 2002, pp. 892–895.

[28] E. U. Onyegam, D. Sarkar, M. Hilali, S. Saha, R. A. Rao, L. Mathew, D. Jawarani, J. Mantey, M. Ainom, R. Garcia, W. James, and S. K. Banerjee, "Exfoliated, thin, flexible germanium heterojunction solar cell with record FF=58.1%," *Sol. Energy Mater. Sol. Cells*, vol. 111, pp. 206–211, Apr. 2013.

[29] T. Kaneko and M. Kondo, "High open-circuit voltage and its low temperature coefficient in crystalline germanium solar cells using a heterojunction structure with a hydrogenated amorphous silicon thin layer," *Jpn. J. Appl. Phys.*, vol. 50, pp. 23–26, Nov. 2011.

[30] G. Attolini, J. S. Ponraj, C. Frigeri, E. Buffagni, C. Ferrari, N. Musayeva, R. Jabbarov, and M. Bosi, "MOVPE growth and characterization of heteroepitaxial germanium on silicon using iBuGe as precursor," *Appl. Surf. Sci.*, vol. 360, pp. 157–163, Jan. 2016.

[31] M. Bosi, G. Attolini, M. Calicchio, C. Ferrari, C. Frigeri, E. Gombia, A. Motta, and F. Rossi, "Homoepitaxial growth of germanium for photovoltaic and thermophotovoltaic applications," *J. Cryst. Growth*, vol. 318, no. 1, pp. 341–344, Mar. 2011.

[32] V. P. Khvostikov, O. A. Khvostikova, P. Y. Gazaryan, S. V. Sorokina, N. S. Potapovich, A. V. Malevskaya, N. A. Kaluzhniy, M. Z. Shvarts, and V. M. Andreev, "Photovoltaic cells based on GaSb and ge for solar and thermophotovoltaic applications," *J. Sol. Energy Eng.*, vol. 129, no. 3, pp. 291–297, Aug. 2007.

[33] Y.-C. Kao, H.-M. Chou, S.-C. Hsu, A. Lin, C.-C. Lin, Z.-H. Shih, C.-L. Chang, H.-F. Hong, and R.-H. Horng, "Performance comparison of III–V//Si and III–V//InGaAs multi-junction solar cells fabricated by the combination of mechanical stacking and wire bonding," *Sci. Rep.*, vol. 9, no. 1, p. 4308, Dec. 2019.

[34] H. Matsubara, T. Tanabe, A. Moto, Y. Mine, and S. Takagishi, "Over 27% efficiency GaAs/InGaAs mechanically stacked solar cell," *Sol. Energy Mater. Sol. Cells*, vol. 50, nos. 1–4, pp. 177–184, Jan. 1998.

[35] A. Sharma, M. Chauhan, V. Bharti, M. Kumar, S. Chand, B. Tripathi, and J. P. Tiwari, "Revealing the correlation between charge carrier recombination and extraction in an organic solar cell under varying illumination intensity," *Phys. Chem. Chem. Phys.*, vol. 19, no. 38, pp. 26169–26178, 2017.

[36] M. K. Hudait, C. L. Andre, O. Kwon, M. N. Palmisiano, S. A. Ringel, and S. Member, "High-performance $In_{0.53}Ga_{0.47}$ as thermophotovoltaic devices grown by solid source molecular beam epitaxy," *IEEE Electron Device Lett.*, vol. 23, no. 12, pp. 697–699, Dec. 2002.

[37] Y. Kim, K. Kim, C. Z. Kim, S. H. Jung, H. K. Kang, W.-K. Park, and J. Lee, "Highly efficient epitaxial ge solar cells grown on GaAs (001) substrates by MOCVD using isobutylgermane," *Sol. Energy Mater. Sol. Cells*, vol. 166, pp. 127–131, Jul. 2017.

[38] A. Belghachi and A. Helmaoui, "Effect of the front surface field on GaAs solar cell photocurrent," *Sol. Energy Mater. Sol. Cells*, vol. 92, no. 6, pp. 667–672, Jun. 2008.

[39] M. S. Shur, *Handbook Series on Semiconductor Parameters: Si, Ge, C (Diamond), GaAs, GaP, GaSb, InAs, InP, InSb*, vol. 1. Singapore: World Scientific, 1996.

[40] T. J. Coutts, "Review of progress in thermophotovoltaic generation of electricity," *Renew. Sustain. energy Rev.*, vol. 3, no. 2, pp. 77–184, 1999.

[41] X. Liu, T. Tyler, T. Starr, A. F. Starr, N. M. Jokerst, and W. J. Padilla, "Taming the blackbody with infrared metamaterials as selective thermal emitters," *Phys. Rev. Lett.*, vol. 107, no. 4, Jul. 2011, Art. no. 045901.

[42] J. K. Tong, W.-C. Hsu, Y. Huang, S. V. Boriskina, and G. Chen, "Thin-film 'thermal well' emitters and absorbers for high-efficiency thermophotovoltaics," *Sci. Rep.*, vol. 5, no. 1, pp. 1–12, Sep. 2015.

[43] P. M. Fourspring, D. M. DePoy, T. D. Rahmlow, J. E. Lazo-Wasem, and E. J. Gratrix, "Optical coatings for thermophotovoltaic spectral control," *Appl. Opt.*, vol. 45, no. 7, pp. 1356–1358, 2006.

[44] Z. Omair, G. Scranton, L. M. Pazos-Outón, T. P. Xiao, M. A. Steiner, V. Ganapati, P. F. Peterson, J. Holzrichter, H. Atwater, and E. Yablonovitch, "Ultraefficient thermophotovoltaic power conversion by band-edge spectral filtering," *Proc. Nat. Acad. Sci. USA*, vol. 116, no. 31, pp. 15356–15361, Jul. 2019.

[45] Y. Xu, T. Gong, and J. N. Munday, "The generalized shockley-queisser limit for nanostructured solar cells," *Sci. Rep.*, vol. 5, no. 1, p. 13536, Oct. 2015.

[46] C. Algora and I. Rey-Stolle, *Handbook of Concentrator Photovoltaic Technology*. Chichester, U.K.: Wiley, 2016.

[47] S. Nakano, Y. Takeuchi, T. Kaneko, and M. Kondo, "Influence of surface treatments on crystalline germanium heterojunction solar cell characteristics," *J. Non-Crystalline Solids*, vol. 358, no. 17, pp. 2249–2252, Sep. 2012.

[48] F.-L. Wu, S.-L. Ou, R.-H. Horng, and Y.-C. Kao, "Improvement in separation rate of epitaxial lift-off by hydrophilic solvent for GaAs solar cell applications," *Sol. Energy Mater. Sol. Cells*, vol. 122, pp. 233–240, Mar. 2014.

[49] F. Khan, S. N. Singh, and M. Husain, "Effect of illumination intensity on cell parameters of a silicon solar cell," *Sol. Energy Mater. Sol. Cells*, vol. 94, no. 9, pp. 1473–1476, Sep. 2010.

[50] F. Khan, S.-H. Baek, and J. H. Kim, "Intensity dependency of photovoltaic cell parameters under high illumination conditions: An analysis," *Appl. Energy*, vol. 133, pp. 356–362, Nov. 2014.

[51] E. Cuce, P. M. Cuce, and T. Bali, "An experimental analysis of illumination intensity and temperature dependency of photovoltaic cell parameters," *Appl. Energy*, vol. 111, pp. 374–382, Nov. 2013.

[52] M. R. Alrashidi and M. F. Alhajri, "Parameters estimation of double diode solar cell model," *Eng. Technol.*, vol. 7, no. 2, pp. 93–96, 2013.

[53] D. S. H. Chan, J. R. Phillips, and J. C. H. Phang, "A comparative study of extraction methods for solar cell model parameters," *Solid-State Electron.*, vol. 29, no. 3, pp. 329–337, Mar. 1986.

[54] E. K. Ali, "Study of mathematical method for parameters calculation of current-voltage characteristic of photovoltaic modules," *Int. J. Mech. Eng. Technol.*, vol. 9, no. 11, pp. 1251–1261, 2018.

[55] A. Orioli and A. Di Gangi, "A procedure to calculate the five-parameter model of crystalline silicon photovoltaic modules on the basis of the tabular performance data," *Appl. Energy*, vol. 102, pp. 1160–1177, Feb. 2013.

[56] G. Miao, T. Zhang, Z. Zhang, and Y. Jin, "Extended spectral response in $I_{n0.82}Ga_{0.18}As$/InP photodetector using InP as a window layer grown by MOCVD," *CrystEngComm*, vol. 15, no. 42, pp. 8461–8464, 2013.

[57] J. Nelson, *The Physics of Solar Cells*. Imperial College, U.K.: Imperial College Press, 2003.
[58] H. Lotfi, L. Li, L. Lei, R. Q. Yang, J. F. Klem, and M. B. Johnson, "Narrow-bandgap interband cascade thermophotovoltaic cells," *IEEE J. Photovolt.*, vol. 7, no. 5, pp. 1462–1468, Sep. 2017.
[59] V. P. Khvostikov, J. L. Santailler, J. Rothman, J. P. Bell, M. Couchaud, C. Calvat, G. Basset, A. Passero, O. A. Khvostikova, and M. Z. Shvarts, "Thermophotovoltaic GaSb cells fabrication and characterisation," in *Proc. AIP Conf. Proc.*, vol. 890, 2007, pp. 198–207.
[60] L. C. Andreani, A. Bozzola, P. Kowalczewski, M. Liscidini, and L. Redorici, "Silicon solar cells: Toward the efficiency limits," *Adv. Phys., X*, vol. 4, no. 1, Jan. 2019, Art. no. 1548305.
[61] T. Burger, D. Fan, K. Lee, S. R. Forrest, and A. Lenert, "Thin-film architectures with high spectral selectivity for thermophotovoltaic cells," *ACS Photon.*, vol. 5, no. 7, pp. 2748–2754, Jul. 2018.
[62] C. Shemelya, D. F. DeMeo, and T. E. Vandervelde, "Two dimensional metallic photonic crystals for light trapping and anti-reflective coatings in thermophotovoltaic applications," *Appl. Phys. Lett.*, vol. 104, no. 2, Jan. 2014, Art. no. 021115.
[63] R. Sharma, A. Gupta, and A. Virdi, "Effect of single and double layer antireflection coating to enhance photovoltaic efficiency of silicon solar," *J. Nano- Electron. Phys.*, vol. 9, no. 2, pp. 02001-1–02001-4, 2017.
[64] F. H. Alharbi, S. N. Rashkeev, F. El-Mellouhi, H. P. Lüthi, N. Tabet, and S. Kais, "An efficient descriptor model for designing materials for solar cells," *NPJ Comput. Mater.*, vol. 1, no. 1, p. 15003, Dec. 2015.

MANSUR MOHAMMED ALI GAMEL received the B.Eng. degree (Hons.) in electrical and electronic engineering from Universiti Tenaga Nasional (UNITEN), Malaysia, in 2018, where he is currently pursuing the M.Eng. degree. He is currently a Research Assistant with the Innovation and Research Management Centre (IRMC), UNITEN. He is also working with Research and Development Sdn. Bhd. to investigate the InGaAs Thermophotovoltaic cell for waste heat-electricity conversion in thermal power plant. His special areas of expertise involve fabrication, and simulation and characterization of photovoltaics and thermophotovoltaics cells. His interests include photovoltaics, thermophotovoltaics, optical sensing, power electronics, and microgrid systems.

PIN JERN KER (Member, IEEE) received the B.Eng. degree (Hons.) in electrical and electronic engineering from Universiti Tenaga Nasional (UNITEN), Malaysia, in 2009, and the Ph.D. degree in electronic and electrical engineering from The University of Sheffield, U.K. From 2016 to 2019, he was seconded with the Institute of Power Engineering, a Research Institute of UNITEN, and the Head of the Unit (Electronics and IT). He is currently a Senior Lecturer with the Department of Electrical Power Engineering, UNITEN. Since April 2019, he has been a Principal Researcher with the Institute of Sustainable Energy, UNITEN. His research interests include simulation and characterization of photodetectors, optical sensing, design of monitoring, and intelligent control system for energy related applications.

WAN EMILIN SULIZA WAN ABDUL RASHID (Member, IEEE) received the B.Eng. degree (Hons.) in chemical engineering from Universiti Teknologi MARA (UiTM), Shah Alam, in 2016, and the master's degree in electrical engineering from Universiti Tenaga Nasional (UNITEN), in 2020. She worked as a Research Engineer with UNITEN Research and Development Sdn. Bhd. under "Investigation of InGaAs Thermophotovoltaic Cell for Waste Heat-Electricity Conversion in Thermal Power Plant" project. Her research interests include simulation, fabrication, and characterization of high efficiency thermophotovoltaic cells for heat-electricity conversion applications.

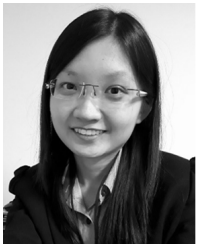

HUI JING LEE (Member, IEEE) received the bachelor's degree in electrical engineering from McGill University, Canada, in 2014, and the master's degree in electrical engineering from Universiti Tenaga Nasional (UNITEN) Malaysia, in 2016, where she is currently pursuing the Ph.D. degree. She is currently working as a Lecturer with the Faculty of Engineering, UNITEN. She was a recipient of the Young Scientist Network-Academy of Sciences Malaysia (YSN-ASM) Young Investigator Award, in 2016.

M. A. HANNAN (Senior Member, IEEE) received the B.Sc. degree in electrical and electronic engineering from the Chittagong University of Engineering and Technology, Chittagong, Bangladesh, in 1990, and the M.Sc. and Ph.D. degrees in electrical, electronic, and systems engineering from the National University of Malaysia (UKM), Bangi, Malaysia, in 2003 and 2007, respectively. He was with UKM, where he became a Senior Lecturer, in 2008, an Associate Professor, in 2010, and a Full Professor, in 2013. He has been a Professor of Intelligent Systems with the Department of Electrical Power Engineering, College of Engineering, The Energy University (UNITEN), Malaysia, since September 2016. He has more than 28 years of industrial and academic experience. He has authored or coauthored around 300 articles published in international journals and conference proceedings. He was received several IEEE best paper awards. He is an Associate Editor of IEEE Access, an Editorial Board Member of many journals, and the Organizing Chair for many conferences.

MD. ZAINI BIN JAMALUDIN (Senior Member, IEEE) received the Diploma degree in electrical and electronic engineering from Institute Technology Mara, University Technology Mara (UiTM), in 1983, the B.Sc. degree in electrical engineering from the University of Miami, Coral Gables, FL, USA, in 1986, the M.Sc. degree in electronic (medical system) from the University of Hertfordshire, U.K., in 1994, and the Ph.D. degree in network communication engineering from Universiti Putra Malaysia, in 2007.

He was a Lecturer with Universiti Technology MARA (UiTM), from 1990 to 1998. Since 2001, he has been a Professor of Photonics with Universiti Tenaga Nasional (UNITEN). He has vast industrial experience having worked in various company, such as Motorola Malaysia, Malaysian e-government network service provider, and Digicert Sdn. Bhd to set-up the first Certification Authority, where his last position was as a Chief Operating Officer in DIGICERT. At UNITEN he was seconded with UNITEN Research and Development and was responsible in setting up the Spin-off company that undertake Research and Development and the Managing Director of URND, from 2013 to 2017. He is an Active Researcher of more than RM8.5 million worth of research grants and consultancy secured from various research funding and agencies, such as Ministry of Higher Education (LRGS, eScience Fund, IRPA, PRGS), TNB Research (TNBR), MCMC, and JICA. He has authored and coauthored more than 100 research papers in journals and conference proceedings. His research interests include photonics devices and sensors, optical network, secured remote data acquisition systems, RF radiation (GSM, Mobile base station), and Ethernet passive optical networks.

Prof. Jamaludin has been a member of IET, since 2010, and an Active Executive Committee Member of the IEEE Photonics Society of Malaysia, International Conference on Photonics (ICP), since 2004. He was a member of IEEE Malaysia for the past 15 years. He was a Conference Chairmen as well as committee members, including as Chairman, from 2007 to 2008. He received his Professional Engineer status, in 2015.